LA-UR- 98-3429

CONF-980842--

Title: Coherent Synchrotron Radiation Experiments for the LCLS

Author(s): Bruce E. Carlsten and Steven J. Russell

Submitted to:

Los Alamos
NATIONAL LABORATORY

DISCLAIMER

Coherent Synchrotron Radiation Experiments for the LCLS

Bruce E. Carlsten and Steven J. Russell

Los Alamos National Laboratory, Los Alamos, NM 87545

We describe a coherent synchrotron radiation experiment planned at Los Alamos to support the design of the Linac Coherent Light Source (LCLS) x-ray FEL. Preliminary simulations of the LCLS compressors show that a clever tuning strategy can be used to minimize the electron's beam emittance growth due to noninertial space-charge forces by employing a delicate cancellation of these forces. The purpose of the Los Alamos experiment, using a sub-picosecond chicane compressor, is to benchmark these simulations tools. In this paper, we present detailed numerical simulations of the experiment, and point out unique signatures of this effect that are measurable. As predicted previously, the largest emittance growths and induced energy spreads result from the nonradiative components of this space-charge force.

I. Introduction

Coherent synchrotron radiation and the related noninertial space-charge force have been identified as potential sources of unacceptable emittance growth for the Linac Coherent Light Source (LCLS) x-ray FEL [1]. Present simulation models, using a clever tuning strategy, show that the emittance growth from this effect can be made tolerable [2]. However, since this effect is potentially so important and the tuning scheme is based on a delicate cancellation of forces, a small experimental program has been initiated to measure both the coherently radiated power and the resulting emittance growth of the electron beam. This experiment will use a low-energy magnetic compressor at Los Alamos National Laboratory, on the Sub-Picosecond Accelerator (SPA) [3]. The experimental results will be then used to verify the models in the design codes used for the LCLS compressors.

This effect has been discussed both analytically and numerically several times [4-10], and its accurate numerical modeling is crucial for the design of the next generation x-ray FELs, but an experiment has not been performed yet that can unambiguously confirm the numerical predictions.

Using the SPA accelerator, we can make such an unambiguous measurement. In the following sections, we will describe (1) the accelerator and compressor, (2) the numerical model used for the coherent synchrotron radiation simulations, and (3) detailed simulations of the experiment. Even at a modest bunch charge of 1 nC, we predict emittance growths of nearly 100% from this effect – at the nominal operating bunch charge of 3 nC, we predict emittance growths of over 300%. Because of the correlated nature of the emittance growth, the emittance growth is not the most when the compressed current is the highest; instead, a rather unique signature in the emittance-versus-bend angle plot is exhibited. In addition, the energy spread induced in the electron bunch that is caused by this effect leads to a decrease in the peak current. Also, the nonradiative part of this space-charge force is mostly responsible for both the decrease in the peak current and the emittance growth.

For the first time, detailed descriptions of electron bunch behavior in an actual magnetic compressor under the influence of this force are presented. Much of the behavior is not intuitive, but can be explained by considering the effect on the energy spread of the beam.

II. Sub-Picosecond Accelerator

The SPA (Fig. 1) has an 8-MeV, 1.3-GHz photoinjector, followed by a four-dipole chicane magnetic compressor. This setup has previously compressed as large a bunch charge as 1.1 nC to a rms bunch length of about 300 fs [11]. The accelerator was originally designed to compress 3 nC to a peak current of 4.5 kA, but during the compressor experiments, a low quantum efficiency of the cathode kept the bunch charge to about 1 nC. (A higher quantum efficiency cathode has been installed for these experiments, allowing operation at 3 nC, if necessary).

Because of unavoidable nonlinearities in the energy-phase correlation of the bunch due to wakefields and the rf curvature, the design of the compressor had to include second-order effects. As a result, the second-order dispersion of the compressor is designed to cancel the second-order curvature in the energy-phase correlation of the bunch entering into the compressor, and the resulting, compressed, bunch length is dominated by the third-order curvature in the initial energy-phase correlation [3]. In order to manipulate the second-order energy-phase correlation, the initial bunch length must be large (about 20 ps FWHM). Additionally, a large bend angle is used in the compressor (about 40 degrees) to generate the required second-order dispersion. In addition to providing second-order compression, use of this large bend angle accentuates the emittance growth from the coherent synchrotron radiation and related effects. Also, the long initial bunch length leads to an initial bunch emittance that is dominated by rf effects, and only weakly dependent on the bunch charge.

III. Model for the space-charge force in bend

For the numerical simulation of this compression experiment, we use a model previously reported [3,12], and quickly summarized here. At an observer location, the total space charge force along the direction of motion from a short, uniform-density line of charge undergoing circular motion is given by [3]

$$E_\theta = \frac{\lambda}{4\pi\varepsilon}\frac{1}{r_{ret} - \vec{r}_{ret}\cdot\vec{u}_{ret}/c}\left(\frac{1}{\gamma^2} - \beta^2\frac{x}{R} + \beta^2\frac{r}{R}(1-\cos\zeta')\right)\Bigg|_{\zeta_r}^{\zeta_f} , \qquad (1)$$

where θ is the direction of motion, R is the radius of curvature of the circular motion, β is the azimuthal velocity divided by the speed of light c, λ is the current density, x is the transverse displacement of the observer location in the bend plane relative to the trajectory of the source line (we can additionally identify y as the displacement in the perpendicular direction), $\vec{r}_{ret}$ is the vector from the source point (presently at azimuthal angular position ζ) at the retarded time to the observer location, $\vec{u}_{ret}$ is the retarded velocity of the source particle at that time, ζ' is the retarded angle of the source point's azimuthal position, and ζ_f and ζ_r are the present azimuthal angles of the front and the rear of the bunch, respectively (where ζ' and ζ are considered positive if they lie behind the observer position). The retarded position ζ' in turn must satisfy the transcendental equation

$$\beta^2 R^2(\zeta' - \zeta)^2 = x^2 + y^2 + 2R(R+x)(1-\cos\zeta') \ . \qquad (2)$$

For sufficiently azimuthally separated observer and source locations, the retarded angle is approximated by $\zeta' = \sqrt[3]{24\zeta}$. Equations (1) and (2) fully specify the problem. Only the force along the direction of motion needs to be considered, because it dominates the effect on the electron particle motion. This model has been incorporated in the ray-tracing code PARMELA [13], and the results have been described elsewhere [3,12]. The length of each line of charge is assumed to be the rms bunch length divided by the cube root of the number of simulated particles. This numerical model correctly predicts both total radiated power along with the proper scalings with bunch length and bend radius, as compared to standard analytic formulas [14]. This model is also stable in terms of number of simulated particles.

Note the three distinct terms in the parenthesis in Eqn. (1). The first, with the $1/\gamma^2$ scaling, is related to the usual straight-line space-charge force, which vanishes at high energy. The second term is known as the noninertial space-charge (NISC) force, which is nonradiative. It vanishes if the bunch has no transverse thickness; unfortunately, in a compressor, the act of compression requires dispersion and thus some transverse thickness. This force is extremely short ranged, and will not be suppressed by any shielding techniques. In addition, the beam can be thought of as having four separate quadrants in x-z space (x positive or negative, z either in front of or behind the bunch centroid). Quadrants diagonally related will have the same induced energy change – thus particles at the same z location but with opposite signs of x will have energy changes in different directions. This symmetry leads to the suppression of radiation, but introduces a problematic correlation in the beam. The third term leads to a radiative force, commonly known as the coherent synchrotron radiation (CSR) force. This force is relatively independent of transverse bunch size, is a long-range force, and results in a decrease in the particles' energy that is mostly monotonic from the head of the bunch to the tail. The short range contribution of the CSR force is relatively small, and use of the approximation $\zeta' = \sqrt[3]{24\zeta}$ does not lead to any appreciable error in the simulation.

IV. PARMELA simulations of the compression experiment

Three types of PARMELA simulations of the compression experiment were done in this study, all using 2000 simulation particles. First, the standard, straight-line space-charge routine was used, even for particle motion within the bends. Next, simulations including the modified standard and the CSR forces for particle motion within the bends were made, using the approximation $\zeta' = \sqrt[3]{24\zeta}$ for the retarded angle. Finally, the full form of Eqn. (1) was used for motion in the bends, including the noninertial space-charge force. For these simulations, Eqn. (2) had to be solved for each pair of particles individually at each time step. A relatively fast root solver was used, but this calculation was much longer than the previous two. The first, simplified, calculations took about 5 minutes on a 300-MHz PC per case, the CSR calculations took about 40 minutes, and the full simulations took about 4 hours.

A bunch charge of 1.1 nC was used, with the same beam characteristics as that reported in the compression experiment [11]. Because of the long initial bunch length, the initial beam emittance was about 11.8 mm mrad entering the compressor. The simplified simulations indicated that a maximum current compression to 1.15 kA should occur at a bend angle of 28 degrees, with a compressed bunch normalized rms emittance of about 12.3 mm mrad. In Figs. 2 and 3 we show simulation results from all three types of simulations, where the solid line is for the simplified simulation, the dashed line is for the CSR simulation, and the dot-dashed line is for the full simulation. In Fig. 2, we see that the CSR force by itself does not appreciable change the compressed peak current (the deviations between the solid and dashed lines is due to the discrete binning of the particles in the post-processor). However, the NISC force does significantly reduce the compressed peak current, by nearly 20%. In Fig. 3, we see that the CSR force by itself increases the compressed bunch emittance by about 20%; however, the NISC force nearly doubles the compressed emittance. A particularly significant signature of the NISC force emittance growth is that the peak of the emittance growth (26 degree bend angle) occurs before the peak of the compressed current (29 degree bend angle). This results from the correlations in the energy spread induced by the NISC force, and partial cancellation as the bunch begins to flip around axially. In Figs. 4, 5, and 6, we present the energy-phase plots of the compressed beam for the simplified, CSR, and full simulations, respectively. Note that the effect of the CSR is to modify the curvature of the energy-phase correlation somewhat, but not to introduce an instantaneous energy spread (since the transverse position leads to little variation in the CSR wake potential). However, the energy-phase correlation is significantly thickened by the NISC force, because of its strong dependence on transverse position, which results in a lower compressed current.

For this case, as well as for the LCLS compressors, the NISC force will lead to a dominant effect. The NISC was also shown to be dominant for the induced energy spread in a long wiggler [12]. The NISC force will leave unambiguous signatures on the peak current and induced emittance growth, and should be unambiguously measured. The simulation model presented earlier in the paper can be confirmed by comparison to measurements, including scalings with beam energy, size, and combinations of initial energy-phase correlations and bend angles.

If, for some reason, there are additional emittance growth mechanisms in the experiment which mask the emittance growth from the CSR and NISC forces (say from some residual axial magnetic field on the cathode or unknown quadrupole nonlinearities), a 3-nC bunch charge can be used. Simplified simulations predict that the initial emittance should be about 14.4 mm mrad (recall that the initial emittance is dominated by rf effects), and that the bunch should be compressed to about 3.8 kA with a final emittance of about 22.1 mm mrad. PARMELA simulations including the effect of both the CSR and NISC forces indicate that the actual emittance will grow to about 68.9 mm mrad (increase of over 300%), with the same characteristics as we discussed for the 1.1 nC case. This emittance growth will be far above emittances measured before for beams exiting this injector (about 15 mm mrad for 5 nC [15]), and will be easily measured, and the benchmarking study for the CSR and NISC forces can still be made.

V. Discussion

We can conclude that the CSR and NISC forces will be important in bunch compressors, and that incorporating these forces in simulation models is essential for proper design of magnetic compressors. In particular, the proposed scheme for the LCLS compressors, in which the transverse kick caused by the energy-spread induced in the first compressor is canceled by transverse kick from the second compressor, requires detailed understanding of these space-charge forces. It should be noted that at high beam energy, the energy spread induced by the NISC force will not led to an appreciable decrease in peak current, but will lead still lead to an equivalent emittance growth. The transverse displacement of the bunch within the compressor is geometrically related to the amount of compression of the bunch and is energy independent. The effect (at the lower energy of the SPA experiment) of an additional broadening of the instantaneous energy may lead to an easier experimental interpretation of the process and benchmarking.

References:

1. R. Tachyn, J. Arthur, M. Baltay, K. Bane, R. Boyce, M. Cornacchia, T. Cremer, A. Fisher, S.-J. Hahn, M. Hernandez, G. Loew, R. Miller, W. R. Nelson, H.-D. Nuhn, D. Palmer, J. Paterson, T. Raubenheimer, J. Weaver, H. Wiedeman, H. Winick, C. Pellegrini, G. Travish, E. T. Scharlemanm, S. Caspi, W. Fawley, K. Halbach, K.-J. Kim, R. Schlueter, M. Xie, D. Meyerhofer, R. Bonifacio, and L. De Salvo, "Research and development towards a 4.5-1.5 A linac coherent light source (LCLS) at SLAC," *Nucl. Instrum. And Meth. Phys. Res. A*, **375**, p. 274 (1996).
2. Chapter 7 of the LCLS Preliminary Design Report, LCLS Design Report Team, SLAC-1234-98.
3. B. E. Carlsten, "Nonlinear subpicosecond electron-bunch compressor," *Nucl. Instrum. And Meth. Phys. Res. A*, **380**, p. 505 (1996).
4. B. E. Carlsten and T. O. Raubenheimer, "Emittance growth of bunched beams in bends," *Phys. Rev. E*, **51**, p. 1453 (1995).
5. B. E. Carlsten, "Calculation of the noninertial space-charge force and the coherent synchrotron radiation force for short electron bunches in circular motion using the retarded Green's function technique," *Phys. Rev. E*, **54**, p. 838 (1996).
6. M. Dohlus and T. Limberg, "Emittance growth due to wake fields on curved bunch trajectories," *Nucl. Instrum. And Meth. Phys. Res. A*, **393**, p. 490 (1997).
7. M. Dohlus and T. Limberg, "Calculation of coherent synchrotron radiation in the TTF-FEL bunch compressor magnet chicanes," *Nucl. Instrum. And Meth. Phys. Res. A*, **407**, p. 278 (1998).
8. Ya. S. Derbenev, J. Rossbach, E. L. Saldin, and V. D. Shiltsev, "Microbunch radiative tail-head interaction," DESY report TESLA-FEL 95-05, Hamburg, 1995.
9. E. L. Saldin, E. A. Schneidmiller, and M. V. Yurkov, "Analytic treatment of the radiative interaction of electrons in a bunch passing in a bending magnet," *Nucl. Instrum. And Meth. Phys. Res. A*, **407**, p. 112 (1998).
10. J. B. Murphy, S. Krinsky, and R. L. Gluckstern, "Longitudinal wakefield for an electron moving on a circular orbit," *Particle Accelerators*, **57**, 9 (1997).
11. B. E. Carlsten and S. J. Russell, "Subpicosecond compression of 0.1-1 nC electron bunches with a magnetic chicane at 8 MeV", *Phys. Rev. E*, **53**, p. 2072 (1996).

12. B. E. Carlsten and J. C. Goldstein, "Emittance growth of a short electron bunch in circular motion," *Nucl. Instrum. And Meth. Phys. Res. A*, **393**, p. 490 (1997).
13. L. Young, Los Alamos National Laboratory, private communication.
14. J. S. Nodvick and D. S. Saxon, "Suppression of coherent radiation by electrons in a synchrotron," *Phys. Rev.*, **96**, p. 180 (1954).
15. B. E. Carlsten, L. M. Young, M. J. Browman, H. Takeda, D. M. Feldman, P. G. O'Shea, and A. H. Lumpkin, "INEX simulations of experimentally measured accelerator performance at the Los Alamos HIBAF facility," *Nucl. Instrum. And Meth. Phys. Res. A*, **304**, p. 587 (1991).

Figure captions:

1. SPA beamline, showing photoinjector and four-dipole chicane compressor.
2. Peak current versus chicane bend angle. Solid line is from using the standard, straight-line space-charge routine, dashed line is from using only using the CSR contribution, and dot-dashed line is from using both the CSR and NISC contributions in Eqn. (1).
3. Compressed bunch emittance versus chicane bend angle. Solid line is from using the standard, straight-line space-charge routine, dashed line is from using only using the CSR contribution, and dot-dashed line is from using both the CSR and NISC contributions in Eqn. (1).
4. Compressed-bunch energy-phase diagram, from using the standard, straight-line space-charge routine.
5. Compressed-bunch energy-phase diagram, from using the CSR contribution in Eqn. (1).
6. Compressed-bunch energy-phase diagram, from using both the CSR and NISC contributions in Eqn. (1).

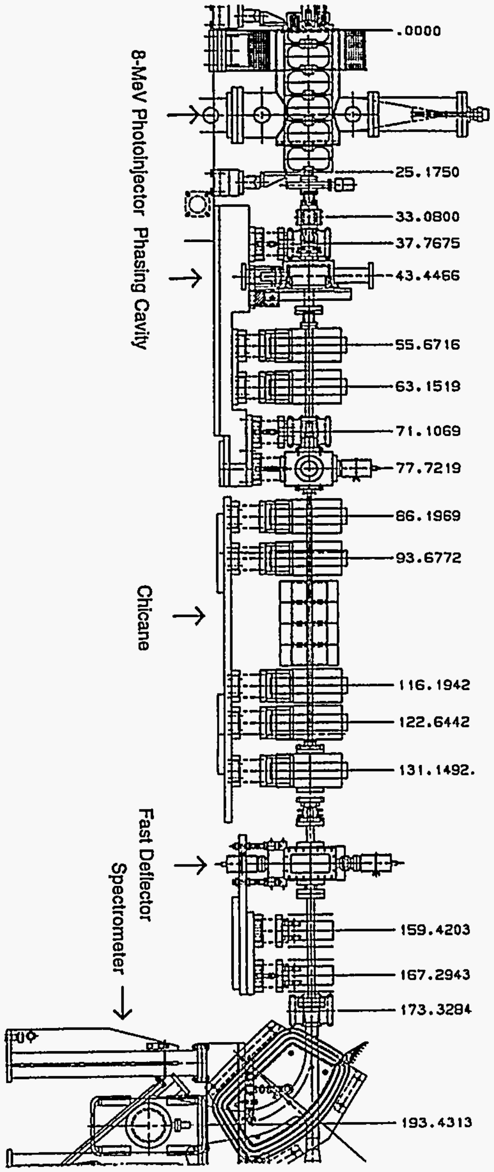
8-MeV PhotoInjector
Phasing Cavity
Chicane
Fast Deflector
Spectrometer
.0000
25.1750
33.0800
37.7675
43.4466
55.6716
63.1519
71.1069
77.7219
86.1969
93.6772
116.1942
122.6442
131.1492.
159.4203
167.2943
173.3284
193.4313

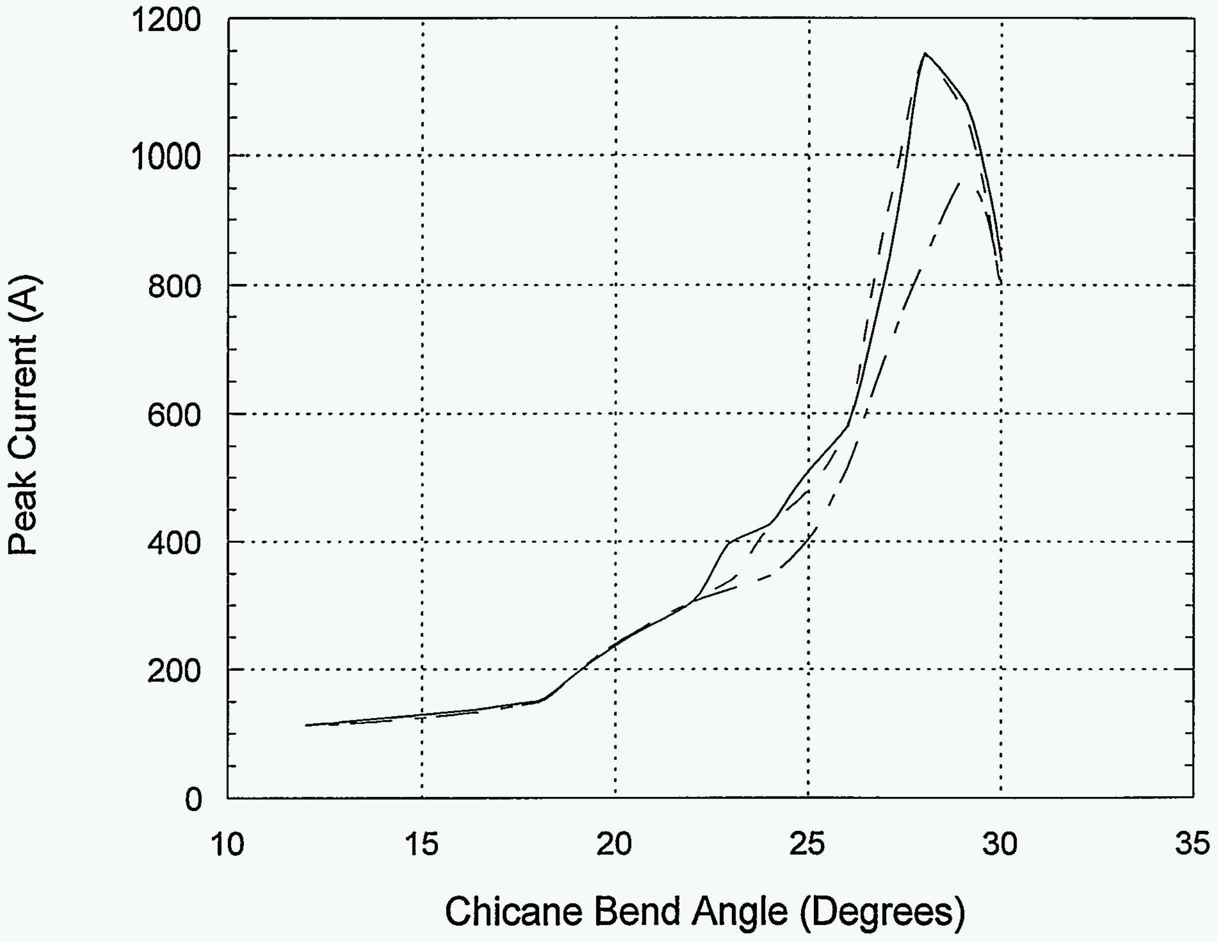
1200
1000
800
600
400
200
0
Peak Current (A)
10
15
20
25
30
35
Chicane Bend Angle (Degrees)

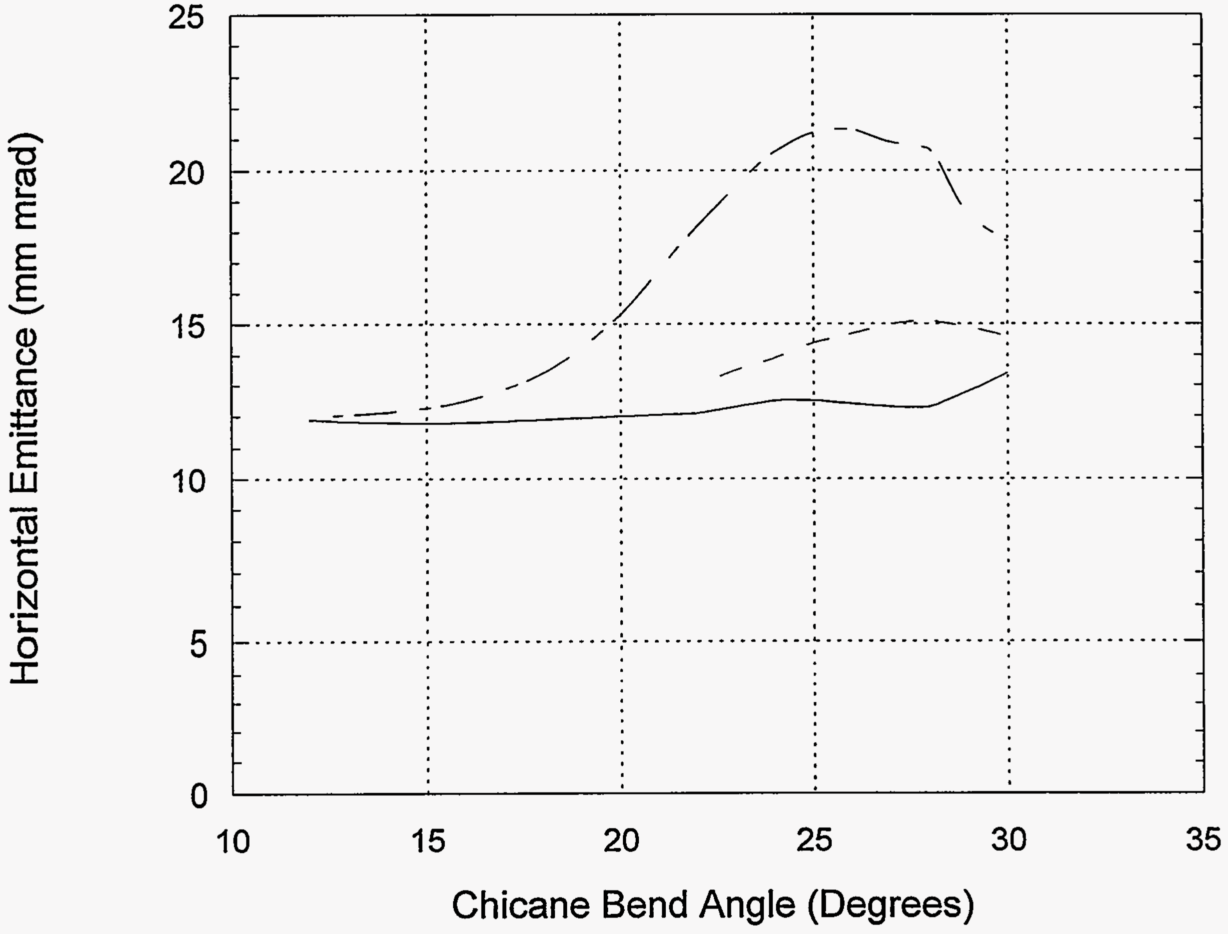
25
20
15
10
5
0
10
15
20
25
30
35
Horizontal Emittance (mm mrad)
Chicane Bend Angle (Degrees)

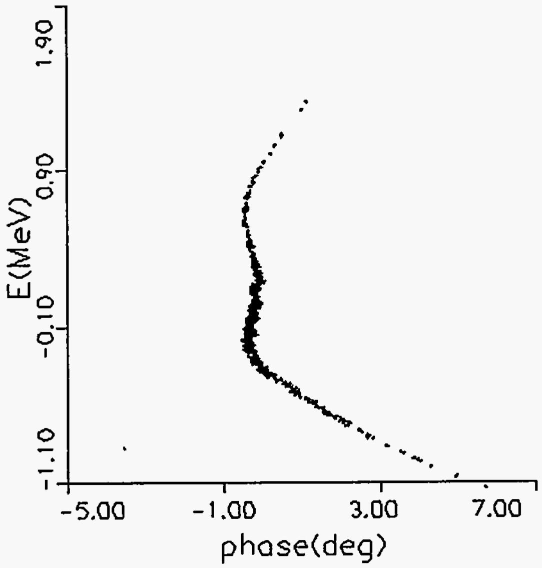
1.90
0.90
-0.10
-1.10
E(MeV)
-5.00
-1.00
3.00
7.00
phase(deg)

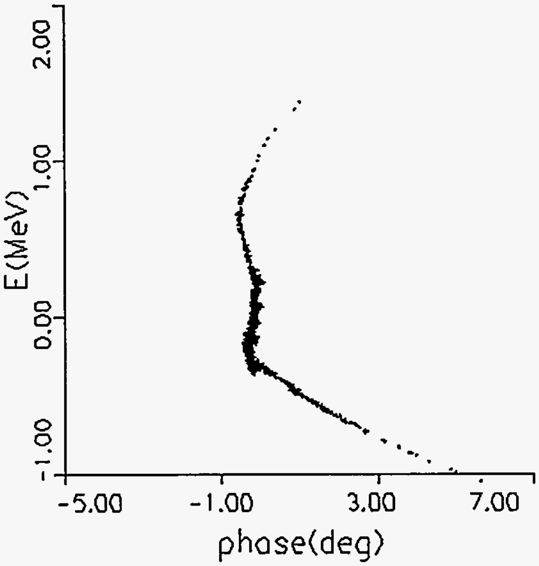
E(MeV)
2.00
1.00
0.00
-1.00
-5.00
-1.00
3.00
7.00
phase(deg)

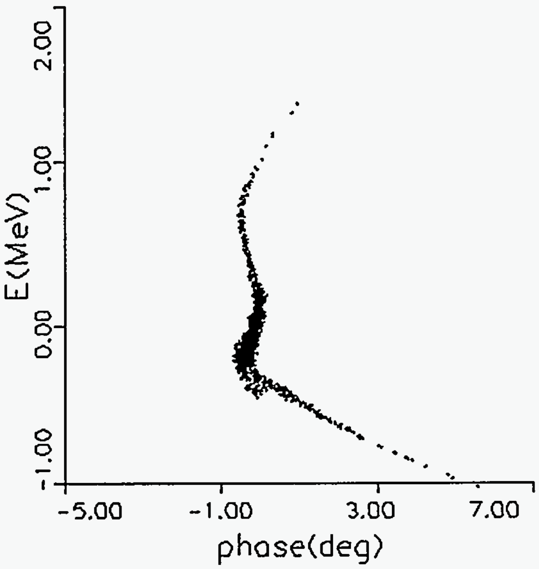
E(MeV)
2.00
1.00
0.00
-1.00
-5.00
-1.00
3.00
7.00
phase(deg)